



ChemComm

**Enhanced mechanical properties of a metal-organic framework by polymer insertion**

Journal:	<i>ChemComm</i>
Manuscript ID	CC-COM-11-2018-008922.R1
Article Type:	Communication

SCHOLARONE™  
Manuscripts



Journal Name

COMMUNICATION

## Enhanced mechanical properties of a metal-organic framework by polymer insertion†

Received 00th January 20xx,  
Accepted 00th January 20xx

Tomoya Iizuka,<sup>a</sup> Kayako Honjo,<sup>b</sup> Takashi Uemura<sup>\*bc</sup>

DOI: 10.1039/x0xx00000x

www.rsc.org/chemcomm

**The mechanical strength of metal-organic frameworks (MOFs) is highly relevant to their practical applications. In this research, we show that encapsulation of polymer chains into MOF nanochannels can effectively restrain the breakage of coordination bonding in MOF and inhibit the amorphization under high physical pressure. The hardness of single MOF crystals was greatly improved, which depended on the direction of inserted polymers, as revealed by nanoindentation analysis. Insertion of polymer chains did not influence the crystal structure of MOFs, which indicates that this approach should be highly promising for improving the mechanical properties of MOFs.**

Metal-organic frameworks (MOFs), which are formed by the self-assembly of metal ions and bridging organic ligands, are a family of nanoporous materials with high structural regularity, so that MOFs have attracted increasing interest in a variety of research fields<sup>1–5</sup>. The porous structures of MOFs (including their size, dimensionality, and surface environment) can be rationally designed, by appropriate choice of the metal ions and bridging linkers, for many useful applications, such as gas storage<sup>6</sup>, molecule separation<sup>7</sup>, catalysis<sup>8,9</sup>, and drug delivery<sup>10</sup>. Despite their remarkable properties, however, they often lack mechanical strength because of the formation of supramolecular structures based on coordination bonding, which is generally weaker than covalent bonding<sup>11</sup>. Irreversible structural collapse of MOFs, including framework distortion, phase transition, and amorphization, is often induced under a high pressure environment, which negatively affects the actual applications of MOFs in industry<sup>12</sup>. Therefore, methods for improving the mechanical strength of MOFs are urgently

required for the further development of MOF science. Obtaining molecular-level insight into the stability of their frameworks is crucial here<sup>13</sup>. In this regard, post-synthetic modification using additional bridging linkers can lead to an increase in the strength of MOF crystals<sup>12,14</sup>. A retrofitting of frameworks can effectively enhance the stability of MOFs under external force. However, this process is always accompanied by the changes in the crystal structure of MOFs, often resulting in the loss of the remarkable functions that are characteristic of the parent frameworks. Another possible approach to overcome this problem is the introduction of guest stiffer molecules into the MOF nanopores, which enhances the mechanical properties without direct modification of the framework structures. However, to date, reports on successful approaches to this guest-induced strengthening are rather limited<sup>15</sup>.

Reinforced concrete is widely used in architectures and buildings because of the increased mechanical strength achieved by reciprocal combination of iron and concrete with high tensile and compressive strengths, respectively<sup>16</sup>. Parallel to this, we now hypothesize that MOF architectures could be highly reinforced by the introduction of molecular chains (polymers) into their nanochannels. Unlike for small molecules, the vapor pressure of polymers is practically nil below their decomposition temperatures, and inserted polymers are not easily extracted from MOFs. In addition, the framework stabilization caused by the polymers would be propagated over the adjacent channels because of the long chain structure. Therefore, even partial loading of polymer chains could increase the mechanical strength of MOFs, without loss of their functions. To date, many types of polymers have been incorporated inside MOFs for the preparation of nanocomposites with synergistic functions<sup>17–19</sup>; however, there are no reports on the mechanical properties of MOF composites accommodating polymers inside the pores. In this research, we introduced polystyrene (PSt) chains into 1D channels of a MOF to investigate the mechanical properties of the host MOF under pressure at the macroscopic and microscopic levels (Fig. 1). The effect of polymer encapsulation

<sup>a</sup> Department of Synthetic Chemistry and Biological Chemistry, Graduate School of Engineering, Kyoto University, Katsura, Nishikyo-ku, Kyoto 615-8510, Japan.

<sup>b</sup> Department of Applied Chemistry, Graduate School of Engineering, The University of Tokyo, 7-3-1 Hongo, Bunkyo-ku, Tokyo 113-8654, Japan. E-mail: t-uemura@k.u-tokyo.ac.jp

<sup>c</sup> CREST, Japan Science and Technology Agency (JST), 4-1-8 Honcho, Kawaguchi, Saitama 332-0012, Japan.

† Electronic Supplementary Information (ESI) available: Experimental procedures, XRPD patterns, N<sub>2</sub> gas adsorption isotherms, SEM images and IR spectra of **1** and **1**⊃PSt, <sup>1</sup>H NMR spectra of before and after polymerization and the results of nanoindentation analysis. See DOI: 10.1039/x0xx00000x

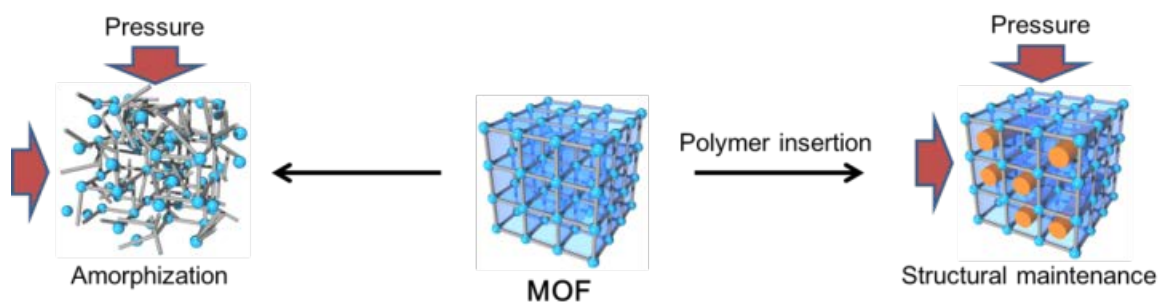


Fig. 1 Schematic illustration of improvement of the mechanical strength by polymer insertion.

on the framework stability was monitored by X-ray powder diffraction (XRPD), scanning electron microscopy (SEM), gas adsorption, and Fourier transform infrared spectroscopy (FT-IR). The nanoindentation technique was used to investigate anisotropic mechanical properties of single crystals of the MOF before and after the introduction of polymer.

Herein, we employed  $[Zn_2(bdc)_2(ted)]_n$  (**1**; bdc = 1,4-benzenedicarboxylate, ted = triethylenediamine), where square grid sheets composed of dinuclear  $Zn_2$  paddle-wheel units and bdc linkers were pillared by ted ligands to form a porous MOF with 1D channels along the [001] direction<sup>20</sup> (Fig. 2). This MOF and its analogs exhibit high gas adsorption capacity<sup>20</sup>, and they have potential for gas separation, based on the hydrophobic pore surface<sup>7</sup>, and for the heterogeneous catalysts of selective reactions<sup>21</sup>. In this study, radical polymerization of styrene in the 1D channels of **1** was performed to introduce PSt chains into the MOF (see Supporting Information, SI).<sup>22</sup> XRPD measurements of the obtained **1**-PSt composite (**1**⊃PSt) and pristine **1** showed that the crystal structure of **1** was maintained during the polymer insertion process (Fig. S2). The amount of PSt encapsulated in **1** was 25 wt%, calculated from <sup>1</sup>H NMR measurements (Fig. S3). Porosity of the composite was inevitably decreased due to the existence of PSt chains inside the nanochannels, showing that the adsorption amount of  $N_2$  was reduced to about a quarter of **1** (from 500 to 130 mg/mL, Fig. S4). Thermogravimetric analysis of **1**⊃PSt showed slight shift of the framework decomposition to higher temperature compared to the original MOF (Fig. S5), implying the stabilization of MOF due to the polymer accommodation.

To study the mechanical stability, we placed pristine **1** and **1**⊃PSt (20 mg) in a 5 mm diameter die and vertically compressed the samples using a hydraulic piston pelletizer (0.37 ton load; 0.18 GPa) (Fig. S6). SEM images revealed that compression of the microcrystals of **1** caused the cuboid crystalline particles to collapse, whereas the morphology of the **1**⊃PSt particles remained relatively unchanged (Fig. S7). Crystalline structure of **1** and **1**⊃PSt was monitored by XRPD,

before and after compression. As shown in Fig. 3, the diffraction peaks for crystalline **1** were hardly observable after the compression treatment of pristine **1**, illustrating the destruction of **1** under 0.18 GPa pressure. In contrast, diffraction peaks for the MOF structure were still detected in the XRPD pattern of the compressed **1**⊃PSt. This indicated that the framework structure of **1** was indeed maintained with PSt, even when high physical pressure was applied. These XRPD results were in good agreement with  $N_2$  gas adsorption measurements of **1** and **1**⊃PSt (Fig. S4). Notwithstanding the accommodation of polymer chains in the nanochannels, the compressed **1**⊃PSt sample exhibited more than double (55 mg/mL) the  $N_2$  adsorption of the compressed **1** (25 mg/mL).

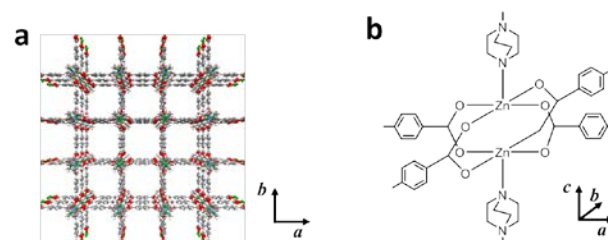


Fig. 2 (a) Crystal structure of **1** (green, red, blue, and white spheres represent Zn, O, N, C and H atoms, respectively.). (b) Coordination geometry of paddle wheel building units in **1**.

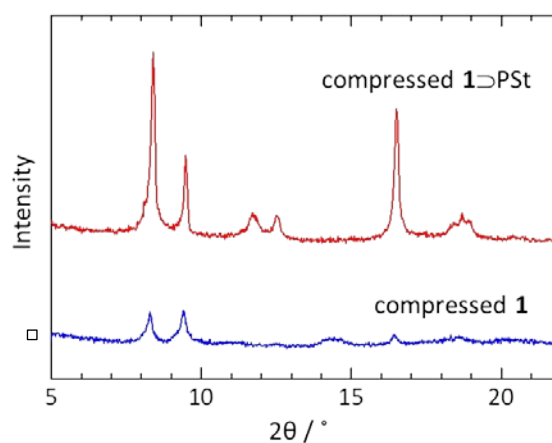


Fig. 3 XRPD patterns of compressed **1** (blue) and **1**⊃PSt (red).

FT-IR analysis gave structural information on the framework stability of **1** after the application of physical pressure (Figs. 4 and S8). In the framework of **1**, the carboxylate group of bdc is coordinated to two Zn ions as a bridging bidentate ligand in a syn-syn configuration. A band found at 1620–1650  $\text{cm}^{-1}$  corresponds to the antisymmetric stretching mode of the carboxylate group<sup>23</sup>. After compression of the pristine **1**, the intensity of this peak decreased considerably, together with the appearance of a broad band at 1550–1600  $\text{cm}^{-1}$ . This result indicated that the compression of only **1** induced bond breaking between Zn and bdc, giving rise to change of the coordination mode for the carboxylate group<sup>13,24</sup>. It is noteworthy that **1**⊃PSt, after the compression, showed the same trend; however, the bond breaking in the MOF was moderate compared with pristine **1**. These results were fairly consistent with those of XRPD and gas adsorption analyses. They revealed that the introduction of PSt chains into **1** effectively inhibits the collapse of the crystalline MOF structure under physical pressure.

To clarify the effect of the polymer introduction on mechanical properties at the nanoscopic level, we performed nanoindentation measurements of **1** and **1**⊃PSt. The nanoindentation technique has been ubiquitously used to analyze the mechanical properties of many materials, including MOFs and polymers, in the micro region<sup>15,25–27</sup>. In this study, we measured the hardness ( $H$ ) of single crystals of **1** and **1**⊃PSt that had sizes of several hundreds of micrometers ( $\mu\text{m}$ ). This

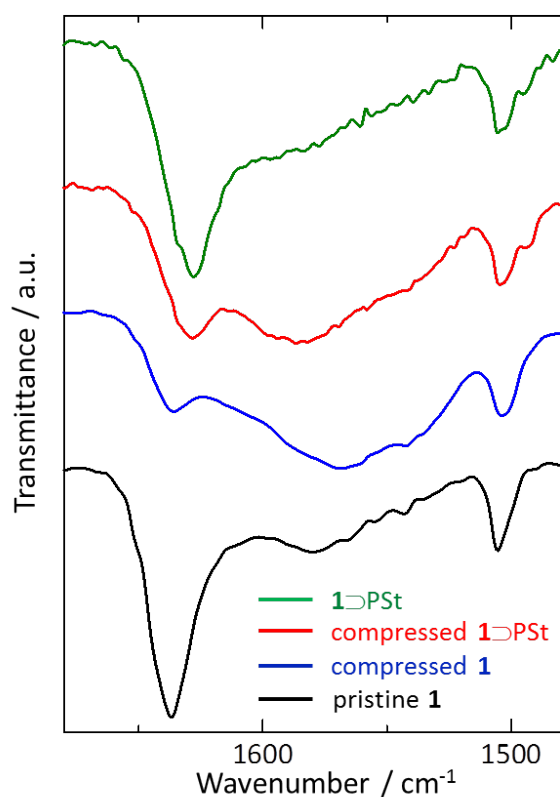


Fig. 4 T-IR spectra of pristine **1** (black), **1**⊃PSt (green) compressed **1** (blue) and **1**⊃PSt (red) in the range of 1680–1480  $\text{cm}^{-1}$ .

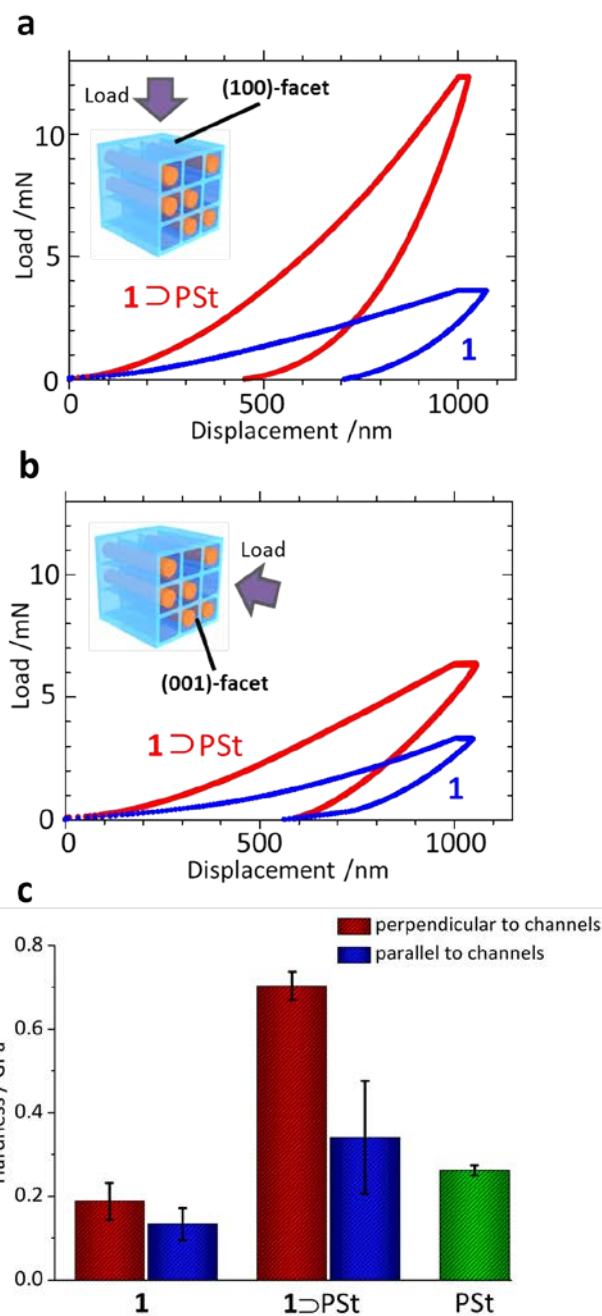


Fig. 5 (a, b) Representative load-displacement curves of single crystal **1** (blue) and **1**⊃PSt (red) in indentation (a) perpendicular and (b) parallel to channels. (c) Values of hardness of **1** and **1**⊃PSt in the indentation perpendicular (red) and parallel (blue) to channels and PSt film.

enabled investigation into the mechanical anisotropy of a crystal of **1** by indentation tests in two different directions, that is, the [100] and [001] directions (perpendicular and parallel to 1D channels, respectively). Hardness can be assumed to express resistance of a material to irreversible plastic deformation<sup>28</sup>. The value of  $H$  was calculated from load-displacement curves, with the maximum indentation depth of 1  $\mu\text{m}$ , using the method of Sawa and Tanaka (see SI for detail

measurement conditions and theory)<sup>29</sup>. A total of 16–32 measurements were carried out for each data point at several different locations on the crystal surfaces of **1** and **1**▷PSt. The representative load-displacement curves of **1** and **1**▷PSt in each direction are shown in Fig. 5a and b. Data summarized in Fig. 5c and Table S1 revealed that *H* of pristine **1** along both the [100] and [001] directions was calculated to be 0.1–0.2 GPa, without showing clear anisotropy in this single crystal. Meanwhile, insertion of PSt in **1** significantly increased *H* of MOF crystals. Tolerance to plastic deformation (*i.e.*, irreversible amorphization) was greatly improved because of the introduction of polymer, which strongly supported the outcome of the pressure application experiment. It is noteworthy that *H* of **1**▷PSt was higher than that of PSt alone (0.262 GPa), indicating the synergistic effect of **1** and PSt on the mechanical strength. Furthermore, introduction of the polymer chains into **1** induced anisotropic mechanical strength enhancement of the single crystals. Indentation of **1**▷PSt along the [100] direction gave a *H* value that was approximately two times larger than that along the [001] direction. This indicated the obvious enhancement of mechanical strength in the direction perpendicular to 1D channels. Although inclusion of small solvent molecules can certainly enhance the mechanical properties of host MOFs,<sup>15</sup> activation of the composites under vacuum results in the removal of the guest molecules, which is essentially problematic for the actual application of MOFs. Introduction of polymer chains into MOFs would be a significant alternative way to enhance the mechanical strength of MOFs with high stability as well as anisotropy.

In summary, we inserted polymer chains into the 1D nanochannels of a MOF and found that there was great enhancement of the mechanical stability of the MOF structure after the application of physical pressure. It is also noteworthy that the anisotropic enhancement of the mechanical strength of MOF crystals was observed in nanoindentation measurement due to 1D accommodation of polymer chains in the frameworks. Generally, the introduction of polymer chains into MOF crystals does not largely affect the original MOF structures. Hence, this procedure should be very useful for strengthening MOFs for their many industrial applications.

This work was supported by the JST-CREST program (JPMJCR1321) and a Grant-in Aid for Science Research on Innovative Area “Coordination Asymmetry” (JP16H06517) from the Ministry of Education, Culture, Sports, Science and Technology, Government of Japan.

## Conflicts of interest

There are no conflicts to declare.

## Notes and references

- J. L. C. Rowsell and O. M. Yaghi, *Microporous Mesoporous Mater.*, 2004, **73**, 3–14.
- Y. Cui, Y. Yue, G. Qien and B. Chen, *Chem. Rev.*, 2012, **112**, 1126–1162.
- L. E. Kreno, K. Leong, O. K. Farha, M. Allendorf, R. P. Van Duyne and J. T. Hupp, *Chem. Rev.*, 2012, **112**, 1105–1125.
- O. Shekhah, J. Liu, R. A. Fischer and C. Wöll, *Chem. Soc. Rev.*, 2011, **40**, 1081–1106.
- P. Ramaswamy, N. E. Wong and G. K. H. Shimizu, *Chem. Soc. Rev.*, 2014, **43**, 5913–5932.
- S. Ma and H.-C. Zhou, *Chem. Soc. Rev.*, 2010, **46**, 44–53.
- Y. F. Chen, J. Y. Lee, R. Babarao, J. Li and J. W. Jiang, *J. Phys. Chem C*, 2010, **114**, 6602–6609.
- D. Farrusseng, S. Aguado and C. Pinel, *Angew. Chem. Int. Ed.*, 2009, **48**, 7502–7513.
- A. H. Chughtai, N. Ahmad, H. A. Younus, A. Laypkov and F. Verpoort, *Chem. Soc. Rev.*, 2015, **44**, 6804–6849.
- R. C. Huxford, J. Della Rocca and W. Lin, *Curr. Opin. Chem. Biol.*, 2010, **14**, 262–268.
- J. C. Tan, T. D. Bennett and A. K. Cheetham, *Proc. Natl. Acad. Sci. U. S. A.*, 2010, **107**, 9938–9943.
- B. Van de Voorde, I. Stassen, B. Bueken, F. Vermoortele, D. De Vos, R. Ameloot, J.-C. Tan and T. D. Bennett, *J. Mater. Chem. A*, 2015, **3**, 1737–1742.
- Z. Su, Y.-R. Miao, G. Zhang, J. T. Miller and K. S. Suslick, *Chem. Sci.*, 2017, **8**, 8004–8011.
- E. A. Kapustin, S. Lee, A. S. Alshammari and O. M. Yaghi, *ACS Cent. Sci.*, 2017, **3**, 662–667.
- S. Henke, W. Li and A. K. Cheetham, *Chem. Sci.*, 2014, **5**, 2392–2397.
- E. G. Perrot, W. L. Webb, C. A. Hexamer, J. Merritt and E. P. Cowell, *J. Franklin Inst.*, 1906, **161**, 1–41.
- T. Uemura, G. Washino, N. Yanai and S. Kitagawa, *Chem. Lett.*, 2013, **42**, 222–223.
- B. Le Ouay, M. Boudot, T. Kitao, T. Yanagida, S. Kitagawa, T. Uemura, *J. Am. Chem. Soc.*, 2016, **138**, 10088–10091.
- T. Uemura, N. Uchida, A. Asano, A. Saeki, S. Seki, M. Tsujimoto, S. Isoda and S. Kitagawa, *J. Am. Chem. Soc.*, 2012, **134**, 8360–8363.
- D. N. Dybtsev, H. Chun and K. Kim, *Angew. Chem. Int. Ed.*, 2004, **43**, 5033–5036.
- L. Peng, S. Wu, X. Yang, J. Hu and X. Fu, *RSC Advances*, 2016, **5**, 72433–72438.
- T. Uemura, K. Kitagawa, S. Horike, T. Kawamura, S. Kitagawa, M. Mizuno and K. Endo, *Chem. Commun.*, 2005, 5968–5970.
- K. Tan, N. Nijem, P. Canepa, Q. Gong, J. Li, T. Thonhauser and Y. J. Chabal, *Chem. Mater.*, 2012, **24**, 3153–3167.
- V. Zelenák, Z. Vargová and K. Györyová, *Spectrochim. Acta A*, 2007, **66**, 262–272.
- B. Bhushan and X. Li, *Int. Mater. Rev.*, 2003, **48**, 125–164.
- M. S. Al-Haik, H. Garmestani, D. S. Li, M. Y. Hussaini, S. S. Sablin, R. Tannenbaum and K. J. Dahmen, *Polym. Sci. B*, 2004, **42**, 1586–1600.
- D. F. Bahr, J. A. Reid, W. M. Mook, C. A. Bauer, R. Stumpf, A. J. Skulan, N. R. Moody, B. A. Simmons, M. M. Shindel and M. D. Allendorf, *Phys. Rev. B*, 2007, **76**, 1–7.
- J. C. Tan and A. K. Cheetham, *Chem. Soc. Rev.*, 2011, **40**, 1059–1080.
- T. Sawa and K. Tanaka, *J. Mater. Res.*, 2001, **16**, 3084–3096.